

THERMAL AND ELECTRICAL CONDUCTANCE OF CARBON NANOSTRUCTURES

David Tománek^a

*Department of Physics and Astronomy
Michigan State University
East Lansing, Michigan 48824-1116, USA*

Abstract

Virtual absence of atomic-scale defects in carbon nanotubes has exciting consequences in terms of their thermal and electrical conductance. The unusually high thermal conductance value of $\lambda \approx 6,600$ W/m·K, predicted for nanotubes at room temperature, exceeds that of any known material, and results from a combination of large phonon mean free path, speed of sound and specific heat. Our electrical transport calculations, performed using a scattering technique based on the Landauer-Büttiker formalism, suggest that the conductance of inhomogeneous multi-wall nanotubes may show an unusual fractional quantization behavior, in agreement with recent experimental data.

Introduction

Carbon nanotubes¹, consisting of graphite layers wrapped into seamless cylinders, are now being produced routinely using carbon arc, laser vaporization of graphite, catalytic decomposition of carbon monoxide at high pressures, and chemical vapor deposition techniques². These methods yield single-wall and multi-wall nanotubes that are up to a

fraction of a millimeter long, yet only nanometers in diameter. Virtual absence of defects suggests that these molecular conductors should be ideal candidates for use as nano-wires that conduct electricity and heat efficiently. There is an increasing interest in such materials that conduct electricity and heat efficiently due to the continually decreasing packing density in electronic and micromechanical devices.

The present study has been motivated by several open questions. The first relates to the suitability of carbon nanotubes to conduct heat efficiently in view of their atomically perfect structure and the stiffness of the interatomic bonds in self-supporting graphitic cylinders. The second open question relates to electron transport in nanotubes that is believed to be ballistic in nature, implying the absence of inelastic scattering. Recent conductance measurements of multi-wall carbon nanotubes³ have raised a significant controversy due to the observation of unexpected conductance values in apparent disagreement with theoretical predictions.

Thermal Conductance of Carbon Nanotubes

To address the thermal conductivity of carbon nanotubes as a function of temperature⁴, we made use of accurate carbon potentials⁵ in equilibrium and non-equilibrium molecular dynamics simulations. The thermal conductivity λ of a solid along a particular direction, taken here as the z axis, is related to the heat flowing down a long rod with a temperature gradient dT/dz by

$$\frac{1}{A} \frac{dQ}{dt} = -\lambda \frac{dT}{dz}, \quad (1)$$

where dQ is the energy transmitted across the area A in the time interval dt . In systems where the phonon contribution to the heat conductance dominates, λ is proportional to Cvl , the product of the heat capacity per unit volume C , the speed of sound v , and the phonon mean free path l . Due to a virtual absence of atomic-scale defects, we expect l to be unusually large in carbon nanotubes. Also the heat capacity and speed of sound are expected to equal or even exceed those of diamond, which is known to have the highest measured thermal conductivity when isotopically pure. Hence, we suspect that isolated carbon nanotubes may be Nature's best heat conductors.

Precise measurements of thermal conductivity are very difficult, as witnessed by the reported thermal conductivity data in the basal plane of graphite⁶ which show a scatter by nearly two orders of magnitude. Similar uncertainties have been associated with thermal conductivity measurements in “mats” of nanotubes⁷.

Theoretical prediction of the thermal conductivity have proven equally challenging, albeit for different reasons. In a direct molecular dynamics simulation, construction of a periodic array of hot and cold regions along a nanotube introduces extra scattering centers that limit the phonon mean free path to below the size of the unit cell, thus significantly reducing the value of λ . Equilibrium molecular dynamics simulations based on the Green-Kubo formula, which relate λ to the integral over time t of the heat flux autocorrelation function, converge very slowly and require extensive ensemble averaging. We found that the most suitable approach to determine thermal conductivity in nanotubes combines the Green-Kubo formula with nonequilibrium thermodynamics^{8,9}.

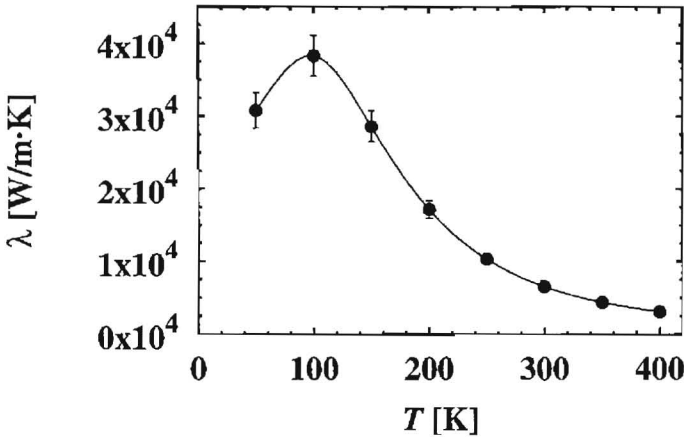


Figure 1: Temperature dependence of the thermal conductivity λ for a (10, 10) carbon nanotube for temperatures below 400 K. (From Ref. [4], ©American Physical Society 2000.)

We found it useful to compare the thermal conductivity of a (10, 10) nanotube to that of an isolated graphene monolayer as well as bulk graphite. For the graphene monolayer, we unrolled the 400-atom large unit cell of the (10, 10) nanotube into a plane. The peri-

odically repeated unit cell used in the bulk graphite calculation contained 720 atoms, arranged in three layers. The results of our calculations, presented in Fig. 2, suggest that an isolated nanotube shows a very similar thermal transport behavior as a hypothetical isolated graphene monolayer, in general agreement with available experimental data^{10–12}. Whereas even larger thermal conductivity should be expected for a monolayer than for a nanotube, we must consider that unlike the nanotube, a graphene monolayer is not self-supporting in vacuum. For all carbon allotropes considered here, we also find that the thermal conductivity decreases with increasing temperature in the range depicted in Fig. 2.

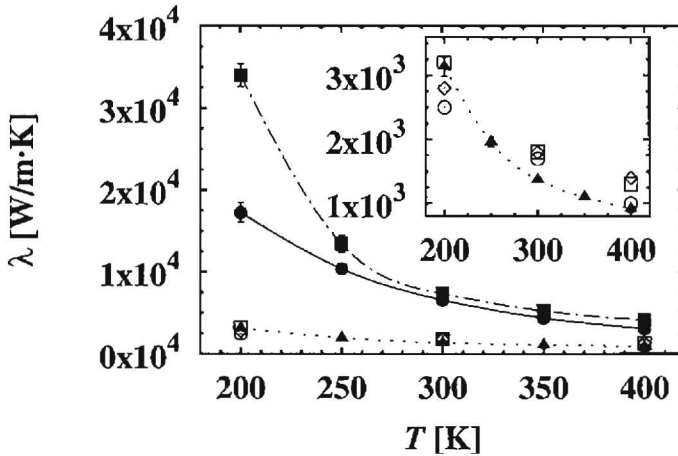


Figure 2: Thermal conductivity λ for a (10,10) carbon nanotube (solid line), in comparison to a constrained graphite monolayer (dash-dotted line), and the basal plane of AA graphite (dotted line) at temperatures between 200 K and 400 K. The inset reproduces the graphite data on an expanded scale. The calculated values (solid triangles) are compared to the experimental data of Refs. [10] (open circles), [11] (open diamonds), and [12] (open squares) for graphite. (From Ref. [4], ©American Physical Society 2000.)

Results of nonequilibrium molecular dynamics simulations for the thermal conductance of an isolated (10,10) nanotube aligned along the z axis are presented in Fig. 1. We find that at low temperatures, when l is nearly constant, the temperature dependence of λ follows that of the specific heat. At high temperatures, where the specific heat is constant, λ decreases as the phonon mean free path becomes smaller due

to umklapp processes. Our calculations suggest that at $T = 100$ K, carbon nanotubes show an unusually high thermal conductivity value of $37,000$ W/m·K. This value lies very close to the highest value observed in any solid, $\lambda = 41,000$ W/m·K, that has been reported¹³ for a 99.9% pure ^{12}C crystal at 104 K. In spite of the decrease of λ above 100 K, the room temperature value of $6,600$ W/m·K is still very high, twice the reported thermal conductivity value of $3,320$ W/m·K for nearly isotopically pure diamond¹⁴. We also found this value to lie close to that of a hypothetical graphene monolayer. In graphite, we find that the inter-layer interaction reduces λ by one order of magnitude due to the reduced phonon mean free path. Similarly, we expect the high thermal conductivity value predicted for an isolated nanotube to decrease upon contact with a surrounding matrix, such as a nanotube “rope”.

Electrical Conductance of Carbon Nanotubes

To address the conductance of multi-wall carbon nanotubes¹⁵, we combined a linear combination of atomic orbitals (LCAO) Hamiltonian with a scattering technique developed recently for magnetic multilayers^{16,17}. The parameterization of the LCAO matrix elements is based on *ab initio* results for simpler structures¹⁸. Our calculations can build on a number of published theoretical studies of the electronic structure of single-wall^{19–21} and multi-wall carbon nanotubes^{22–24}. Calculations for single-wall nanotube ropes^{25,26} have shown that inter-wall coupling may induce pseudo-gaps near the Fermi level in these systems, with serious consequences for their conductance behavior.

Our scattering technique approach to determine the conductance of inhomogeneous multi-wall nanotubes¹⁵ is based on the quantum-mechanical scattering matrix S of a phase-coherent “defective” region that is connected to “ideal” external reservoirs¹⁶. At zero temperature, the energy-dependent electrical conductance is given by the Landauer-Büttiker formula²⁷

$$G(E) = \frac{2e^2}{h} T(E), \quad (2)$$

where $T(E)$ is the total transmission coefficient, evaluated at the Fermi energy E_F .

For a homogeneous system, $T(E)$ assumes integer values corresponding to the total number of open conduction channels at the energy E . For individual (n, n) “armchair” tubes, this integer is further predicted²⁸ to be an even multiple of the conductance quantum $G_0 = 2e^2/h \approx (12.9 \text{ k}\Omega)^{-1}$, with a conductance $G = 2G_0$ near the Fermi level. In the $(10, 10)@(15, 15)$ double-wall nanotube²⁴ and the $(5, 5)@(10, 10)@(15, 15)$ triple-wall nanotube, the inter-wall interaction significantly modifies the electronic states near the Fermi level and blocks some of the conduction channels close to E_F , as shown in Fig. 3.

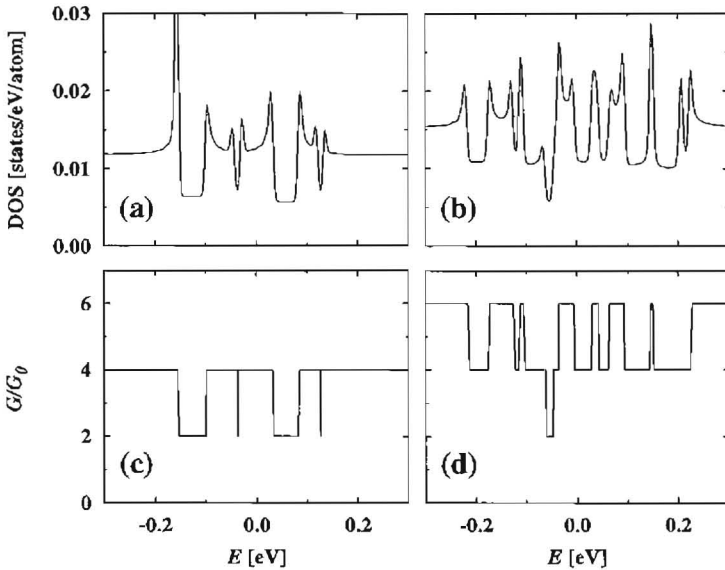


Figure 3: Electronic density of states and conductance of a double-wall $(10,10)@(15,15)$ nanotube [(a) and (c), respectively], and a triple-wall $(5,5)@(10,10)@(15,15)$ nanotube [(b) and (d), respectively]. (From Ref. [15], ©American Physical Society 2000.)

The experimental set-up of Ref. [3], shown schematically in Fig. 4(a), consists of a multi-wall nanotube that is attached to a gold tip of a Scanning Tunneling Microscope (STM) and used as an electrode. The STM allows the tube to be immersed at calibrated depth intervals into liquid mercury, acting as a counter-electrode. This arrangement allows precise conduction measurements to be performed on an isolated tube. The experimental data of Ref. [3] for the conductance G as a function

of the immersion depth z of the tube, reproduced in Fig. 4(e), suggest that in a finite-length multi-wall nanotube, the conductance may achieve values as small as $0.5G_0$ or $1G_0$.

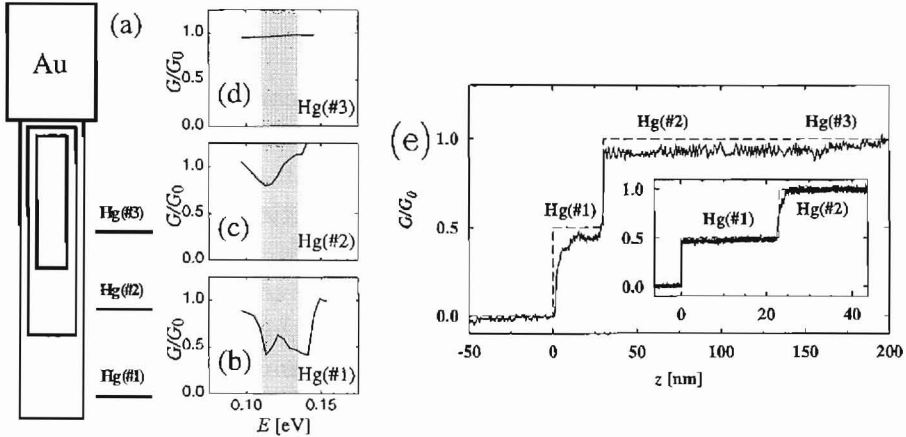


Figure 4: (a) Schematic geometry of a multi-wall nanotube that is being immersed into mercury up to different depths labeled Hg(#1), Hg(#2), and Hg(#3). Only the outermost tube is considered to be in contact with the gold STM tip on which it is suspended. The conductance of this system is given in (b) for the immersion depth Hg(#1), in (c) for Hg(#2), and in (d) for Hg(#3) as a function of the position of E_F . The Fermi level may shift with changing immersion depth within a narrow range indicated by the shaded region. (e) Conductance G of a multi-wall nanotube as a function of immersion depth z in mercury, given in units of the conductance quantum $G_0 = 2e^2/h \approx (12.9 \text{ k}\Omega)^{-1}$. Results predicted for the multi-wall nanotube, given by the dashed line, are superimposed on the experimental data of Ref. [3]. The main figure and the inset show data for two nanotube samples, which in our interpretation only differ in the length of the terminating single-wall segment. (From Ref. [15], ©American Physical Society 2000.)

As nothing is known about the internal structure of the multi-wall nanotubes used or the nature of the contact between the tube and the Au and Hg electrodes, we have considered several scenarios and concluded that the experimental data can only be explained by assuming that the current injection from the gold electrode occurs exclusively into the outermost tube wall, and that the chemical potential equals that of mercury, shifted by a contact potential, only within the submerged portion of the tube. In other words, the number of tube walls in contact with mercury depends on the immersion depth. The main origin of the anomalous conductance reduction from the theoretically

expected integer multiple of $2G_0$ is the backscattering of carriers at the interface of two regions with different numbers of walls due to a discontinuous change of the conduction current distribution across the individual walls.

Summary and Conclusions

The calculations discussed above indicate that carbon nanotubes show unusual electrical and thermal conductance behavior. Results for the electrical transport indicate that the inter-wall interaction in multi-wall nanotubes not only blocks certain conduction channels, but also re-distributes the current non-uniformly across the walls. The puzzling observation of fractional quantum conductance in multi-wall nanotubes can be explained by back-scattering at the interfaces of regions with different numbers of walls. Sample-to-sample variations in the internal structure of the tubes offer a natural explanation for the observed variations of the conductance. Nonequilibrium molecular dynamics simulations suggest that carbon nanotubes may conduct heat exceptionally well, owing to a combination of a large phonon mean free path, high speed of sound and specific heat. The predicted thermal conductivity value $\lambda \approx 6,600$ W/m·K for an isolated (10,10) carbon nanotube at room temperature is twice that of isotopically pure diamond, Nature's best heat conductor.

Acknowledgment

The author gratefully acknowledges financial support by the organizers of the NATO Advanced Study Institute on "Nanostructured carbon for advanced applications" in Erice (Italy), July 19-30, 2000, and by the Office of Naval Research and DARPA under Grant Number N00014-99-1-0252.

References

- ^a In collaboration with Young-Kyun Kwon, Savas Berber, Stefano Sanvito, and Colin J. Lambert.
1. S. Iijima, *Nature* **354**, 56 (1991).
2. M.S. Dresselhaus, G. Dresselhaus, and P.C. Eklund, *Science of Fullerenes and Carbon Nanotubes* (Academic Press, San Diego, 1996).

3. S. Frank, P. Poncharal, Z.L. Wang, and W.A. de Heer, *Science* **280**, 1744 (1998).
4. Savas Berber, Young-Kyun Kwon, and David Tománek, *Phys. Rev. Lett.* **84** (2000).
5. J. Tersoff, *Phys. Rev. B* **37**, 6991 (1988).
6. Citrad Uher, in *Landolt-Börnstein*, New Series, III **15c** (Springer-Verlag, Berlin, 1985), pp. 426–448.
7. J. Hone, M. Whitney, A. Zettl, *Synthetic Metals* **103**, 2498 (1999).
8. D.J. Evans, *Phys. Lett.* **91A**, 457 (1982).
9. D.P. Hansen and D.J. Evans, *Molecular Physics* **81**, 767 (1994).
10. Takeshi Nihira and Tadao Iwata, *Jpn. J. Appl. Phys.* **14**, 1099 (1975).
11. M.G. Holland, C.A. Klein and W.D. Straub, *J. Phys. Chem. Solids* **27**, 903 (1966).
12. A. de Combarieu, *J. Phys. (Paris)* **28**, 951 (1967).
13. Lanhua Wei, P.K. Kuo, R.L. Thomas, T.R. Anthony, and W.F. Banholzer, *Phys. Rev. Lett.* **70**, 3764 (1993).
14. T.R. Anthony, W.F. Banholzer, J.F. Fleischer, Lanhua Wei, P.K. Kuo, R.L. Thomas, and R.W. Pryor, *Phys. Rev. B* **42**, 1104 (1990).
15. Stefano Sanvito, Young-Kyun Kwon, David Tománek, and Colin J. Lambert, *Phys. Rev. Lett.* **84**, 1974 (2000).
16. S. Sanvito, C.J. Lambert, J.H. Jefferson, and A.M. Bratkovsky, *Phys. Rev. B* **59**, 11936 (1999).
17. S. Sanvito C.J. Lambert, J.H. Jefferson, and A.M. Bratkovsky, *J. Phys. C: Condens. Matter.* **10**, L691 (1998).
18. D. Tománek and M.A. Schluter, *Phys. Rev. Lett.* **67**, 2331 (1991).
19. J.W. Mintmire, B.I. Dunlap, and C.T. White, *Phys. Rev. Lett.* **68**, 631 (1992).
20. R. Saito, M. Fujita, G. Dresselhaus, and M.S. Dresselhaus, *Appl. Phys. Lett.* **60**, 2204 (1992).
21. N. Hamada, S. Sawada, and A. Oshiyama, *Phys. Rev. Lett.* **68**, 1579 (1992).
22. R. Saito, G. Dresselhaus, and M.S. Dresselhaus, *J. Appl. Phys.* **73**, 494 (1993).

23. Ph. Lambin, L. Philippe, J.C. Charlier, and J.P. Michenaud, *Comput. Mater. Sci.* **2**, 350 (1994).
24. Y.-K. Kwon and D. Tománek, *Phys. Rev. B* **58**, R16001 (1998).
25. P. Delaney, H.J. Choi, J. Ihm, S.G. Louie, and M.L. Cohen, *Nature* **391**, 466 (1998).
26. Y.-K. Kwon, S. Saito, and D. Tománek, *Phys. Rev. B* **58**, R13314 (1998).
27. M. Büttiker, Y. Imry, R. Landauer, and S. Pinhas, *Phys. Rev. B* **31**, 6207 (1985).
28. L. Chico, L.X. Benedict, S.G. Louie and M.L. Cohen, *Phys. Rev. B* **54**, 2600 (1996), W. Tian and S. Datta, *ibid.* **49**, 5097 (1994), M.F. Lin and K.W.-K. Shung, *ibid.* **51**, 7592 (1995).